Proceedings, 7th African Rift Geothermal Conference
Kigali, Rwanda 31st October – 2nd November 2018

Prospecting For Geothermal Resources Using Thermal Infrared (TIR) Remote Sensing

Charleson Namandwa Eliyasi

Geological Survey of Malawi, P. O. Box 27, Zomba, Malawi.

celiyasi@yahoo.com

Keywords

Malawi, Thermal Infrared, Geothermal springs, Anomalies, Solar irradiation

ABSTRACT

Thermal Infrared (TIR) remote sensing was applied to map surface temperature anomalies related to geothermal activities in the northern part of Malawi. Geothermal surface manifestations such as warm grounds, hot springs, fumaroles and geysers, create surface temperature anomalies that can be mapped using Thermal Infrared (TIR) remote sensing.

ASTER night scene covering Chiweta area, was used for the mapping of geothermal surface temperature anomalies. Night scenes are chosen because they are less influenced by the day time solar irradiation. In addition to that, the thermal infrared (TIR) region of ASTER has five bands (from band 10-14) and has 90m spectral resolution. Such being the case, it is as a useful tool for quantifying and detection of surface temperature.

ENVI classic with IDL was used to run the STcorr.sav software. STcorr is interactive data language (IDL) code for the correction of altitude, aspect and slope effects in thermal imagery, using image based polynomial regression analysis. Basically, the polynomial fit is applied to remove the artefacts that occur at night during cooling. The four images namely; temperature, altitude, slope and aspect were used as input in the STcorr.sav software. The images were masked for water bodies and the degree of polynomial fits were chosen depending on the type of data cloud. For instance, second and third polynomial fit regression operations were done to correct relict illumination effects of diurnal heat which are caused by aspect and slope. From this processing, the temperature images were corrected for altitude, aspect as well as slope and the resulting images were the final corrected thermal images that were almost free from these topographic influences.

The results showed surface temperature anomalies associated with geothermal activities in the area. When ground follow up was conducted in the study area, geothermal surface manifestations in form of hot springs were observed. The method proved to be cost effective and applicable to other geothermal occurrence areas.

1. Introduction

Malawi is located in the southern end of the western arm of the East African Rift System. It lies within latitudes 9^0 S and 17^0 S and longitudes 32^0 E and 36^0 E. It is mainly underlain by basement metamorphic rocks which are mainly intruded by basic granitic and syenite rocks and overlain by sedimentary rocks.

Structurally, the study area (northern Malawi) lies in the apparent meeting point of three major mobile belts that were formed during the three main Orogenic episodes (Ray, 1975). These episodes were associated with rifting and faulting of the crust. The movements resulted into formation of geological structures such as faults which are believed to have a direct bearing on the geothermal occurrences in the area.

Such being the case, the country has a number of geothermal occurrences that are manifested on the surface as warm and hot springs. The northern part of the country has geothermal springs with highest temperatures hence the choice for this study.

2. Study area

The study area is known as Chiweta. It is located in the northern part of Malawi in the Rumphi district (Figure 1) and is bounded by Lake Malawi to the east. The geothermal manifestations are in form of hot springs and it is close to Lake Malawi. It is about 500 m wide and 3 km long, rectangular shaped and oriented in a NW-SE direction. The area is bordered by the Chiweta fault in the north and NNE-SSW, trending fault to the west. The surface temperature is about 79-80^0 C (Ebinger et al., 1987)

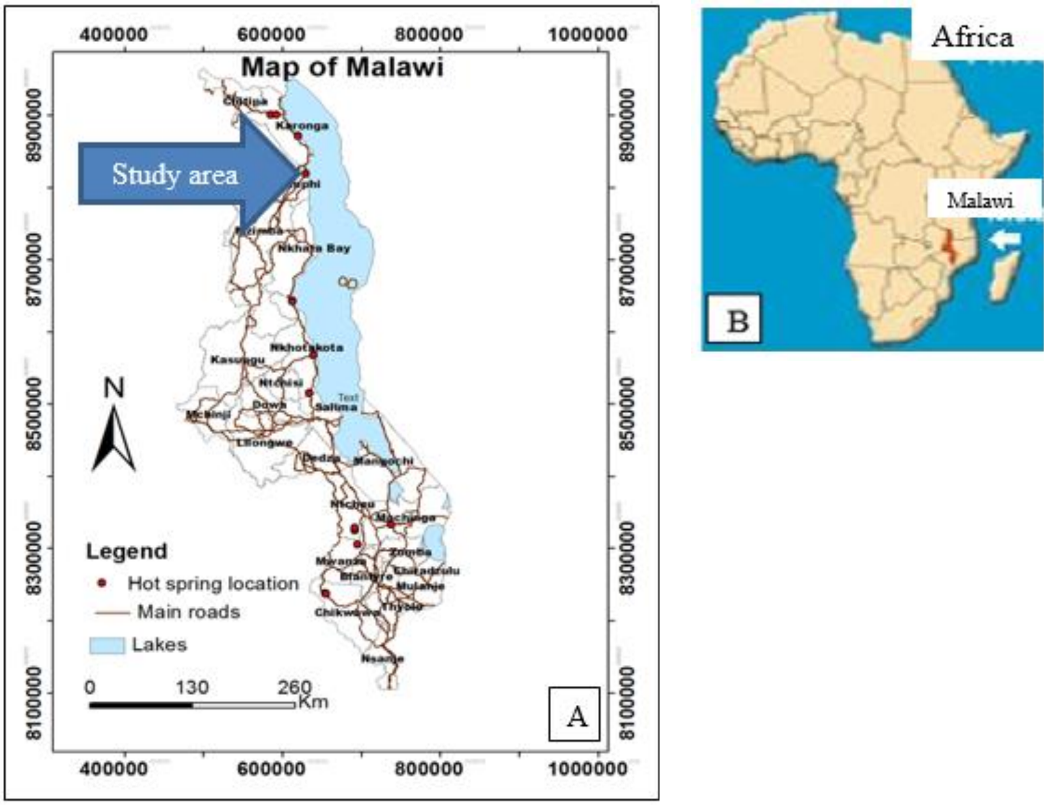

Figure 1 (A&B): Map of Malawi (A) showing the study area and Africa (B) (source-google map, insert) showing location of Malawi (in red)

Thermal Infrared (TIR) remote sensing was applied to map surface temperature anomalies related to geothermal activities in the area. Geothermal surface manifestations such as warm grounds, hot springs, fumaroles and geysers, create surface temperature anomalies that can be mapped by using Thermal Infrared (TIR) remote sensing (Haselwimmer and Prakash, 2013).

A similar technique has been applied in many areas. For instance, Ulusoy et al, (2012) used ASTER TIR to detect hot spots at mount Nemrut in Turkey among others.

3. Methodology

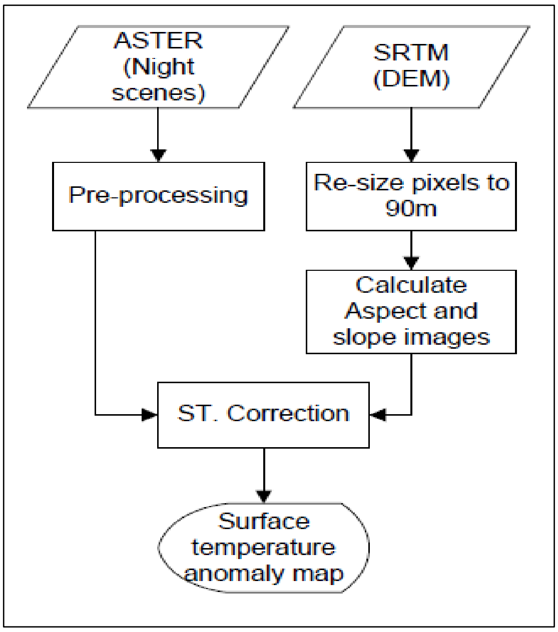

Figure 2: Flow chart

4. Data used and description

ASTER night scene (AST_L1B acquired on 11/10/2009) and Shuttle Radar topographic Mission (SRTM) Digital Elevation Model (DEM) data for the study area were the main input images that were used. Night scenes are suitable for such type of study because they are less influenced by the day time solar irradiation (Ulusoy et al., 2012). In addition to that, the thermal infrared (TIR) region of ASTER has five bands (from band 10-14) and has 90m spectral resolution (Abrams and Hook, 2002). Such being the case, it is considered as a useful tool for quantifying and detection of surface temperature (Haselwimmer and Prakash, 2013). Despite the fact that ASTER night scenes are less influenced by solar irradiation, there are still some residual illumination effects on the surface temperature image that are supposed to be corrected as such, surface temperature correction (STcorr) was applied. Other images that were used such as slope and aspect were generated from the SRTM DEM image.

5. Pre-processing

The first stage in the thermal anomaly mapping was to pre-process the data. Firstly, spatial subset was performed to remove areas of no data from the ASTER image. Then, atmospheric correction was done to the images using the thermal atmospheric correction in ENVI 5.1 software followed by a temperature emissivity separation based on Emissivity normalization. The assumed emissivity value of 0.96 was used and the temperature image was generated.

SRTM image was re-projected from Geographic (latitude-longitude) to Universal Transverse Mercator (UTM) coordinate system, (WGS 1984, and zone 36 south). The temperature and the STRM images were layer stacked to have the same spatial area by using exclusive range only. To avoid black edges after the rotation that comes after layer stacking a mask was made on the layer stack that included all NaN's (not a number) and zeros. Finally altitude, slope and aspect images were prepared using the SRTM image as input (Figures 3, A, B, C, and D)

.

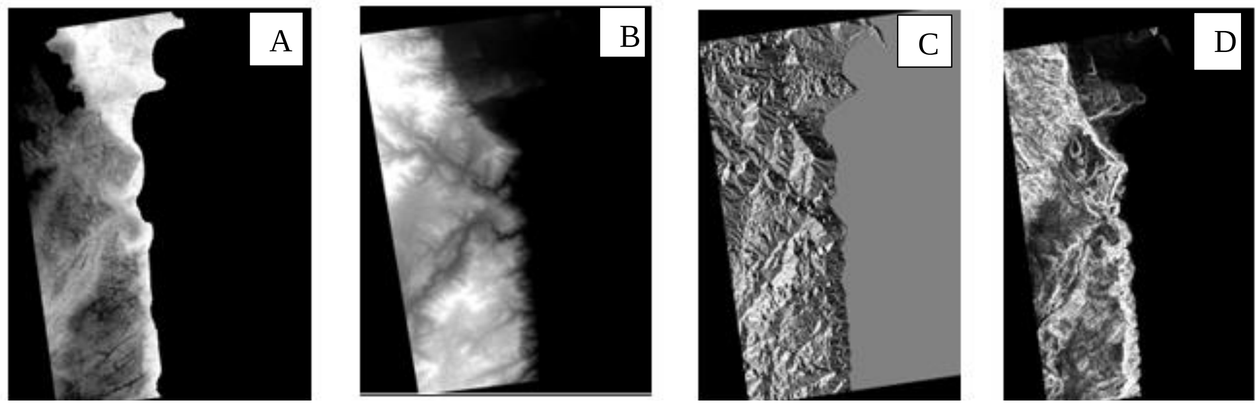

Figure 3: Examples of temperature (A), altitude (B), slope (C) and (D) aspect images used as input in the STcorr.sav software.

5.1. *Application of surface temperature correction*

ENVI classic with IDL was used to run the STcorr.sav software. STcorr is interactive data language (IDL) code for the correction of altitude, aspect and slope effects in thermal imagery, using image based polynomial regression analysis (Ulusoy et al., 2012). Basically, the polynomial fit is applied to remove the artefacts that occur at night during cooling. The four images (Figure 3) namely; temperature (A), altitude (B), slope (C) and aspect (D) were used as input in the STcorr.sav software. The images were masked for water bodies and the degree of polynomial fits were chosen depending on the type of data cloud. For instance, second and third polynomial fit regression operations were done to correct relict illumination effects of diurnal heat which are caused by aspect and slope. From this processing, the temperature images were corrected for altitude, aspect as well as slope and the resulting images were the final corrected thermal images that were almost free from these topographic influences.

5.2 Regression computation for corrections

The regression computations for the correction of the effects of altitude, aspect and slope effects in thermal imagery are based on polynomial fit to the image. The polynomial fits can be fitted from the first to sixth degree depending on the shape of the data cloud. Images of lapse rate, slope and aspect are generated. These help to normalize the thermal anomalies and also enhance the contrast so that the anomalies are more visible.

6. Results

The results showed inverse relationship between temperature and altitude. For instance as the altitude increased temperature decreased (Figures 4 a) The scatter graphs for various ST corr code (Figures 4, a, b, c) showed how aspect, slope and attitude contributed to the correction.

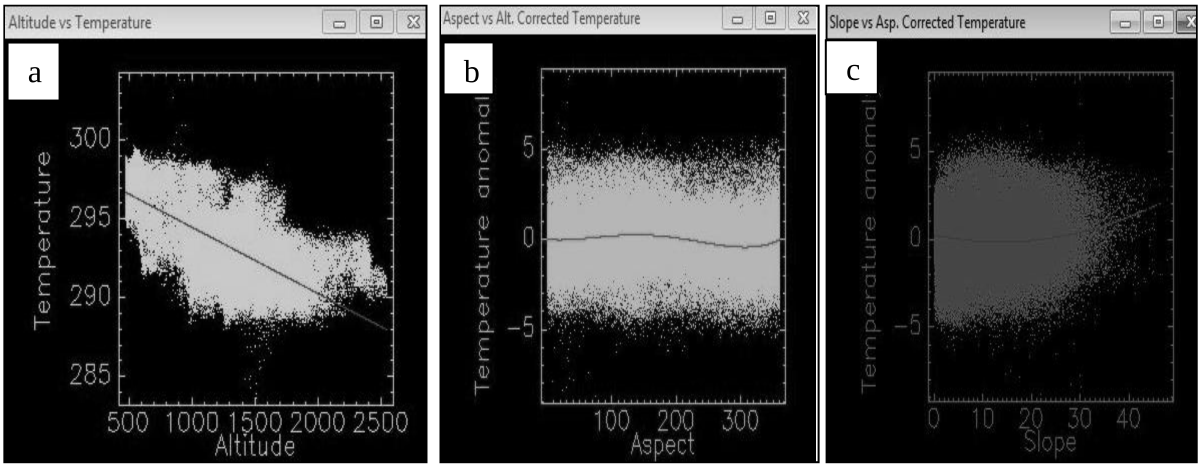

Figure 4: Scatter graphs for various ST corr code for Chiweta area (a) temperature versus altitude, (b) slope and (c) aspect.

After the correction, the resulting image showed thermal anomalies for the study area and a thermal anomaly map was created (Figure 5).

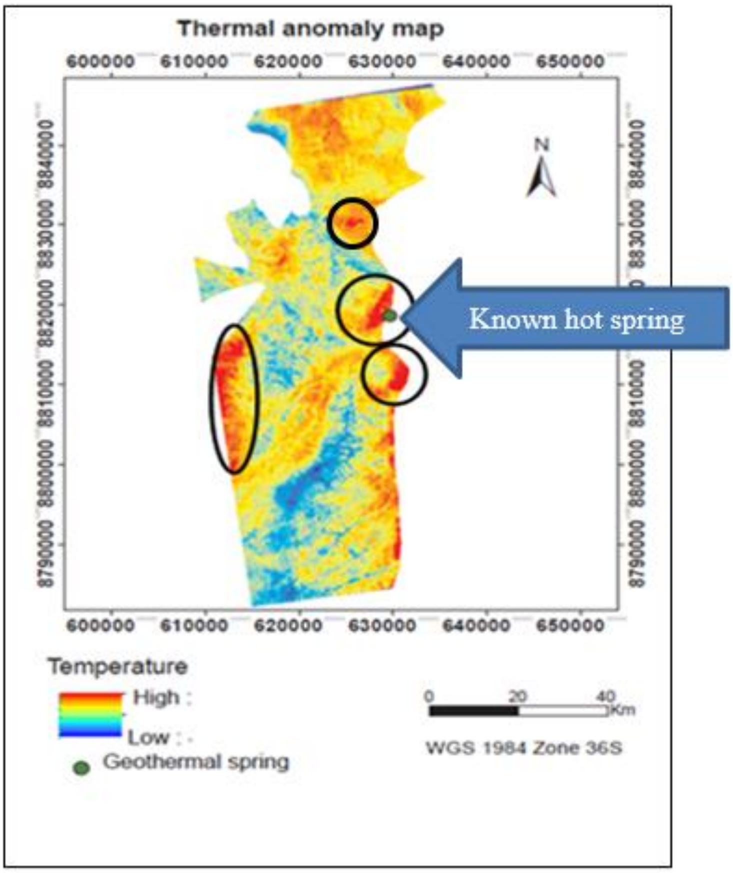

Figure 5: Geothermal surface temperature anomalies for both known geothermal spring location (green dot) and unknown location (in black circles)

7. Discussion

The application of surface temperature correction (STcorr) proved more effective in the sense that, thermal anomalies were observed at Chiweta geothermal area (Figure 5). In addition to that the software used enabled some flexibility to choose the degree of polynomial fit according to the data used. Furthermore the masking of water bodies and other unwanted features enabled the corrected thermal image to be free from the influence of such features. As a result, a Thermal anomaly or surface temperature map for the area was created (Figure 5)

When known geothermal location points were plotted on the image showing the thermal anomalies, they coincided with some of the already known hot spring sites (Figure 5). This demonstrates that, the anomalies that were observed were related to geothermal activities in the area.

Finally, the study area was more favourable for the study because it is wider and has less vegetative cover. Furthermore, the surface temperature for the area ranged from 79-80^{0}C.

8. Limitation of the study.

The main challenge to the method is that in other instances, the resulting images show both thermal anomalies related to geothermal activities and also those that are due to other sources such as forest fires as such, it requires a careful assessment of the anomalies in order to establish whether they are geothermal related or not.

9. Conclusion

The study has shown that Thermal Infrared (TIR) remote sensing can be used as a useful tool for prospecting geothermal resources. The method saves time and is cost effective. In addition, the method is more applicable to areas of similar surface temperature range or above, However, images with less vegetation and clouds are easy to use.

10. REFERENCES

Abrams, M. and Hook. S. (2002). ASTER User Handbook. *Handbook*, *2*, 8–133. Retrieved from http://www.pancroma.com/downloads/aster user guide vs.pdf.

Coolbaugh, M. F., Kratt, C., Fallacaro, a., Calvin, W. M., & Taranik, J. V. (2007). Detection of geothermal anomalies using Advanced Spaceborne Thermal Emission and Reflection Radiometer (ASTER) thermal infrared images at Bradys Hot Springs, Nevada, USA. *Remote Sensing of Environment*, *106*(3), 350–359. doi:10.1016/j.rse.2006.09.001

Ebinger C.J, Rosendahl, B. R. and, & Reynolds, D. J. (1987). Tectonic model of the MalaW rift , Africa.Retreaved from http://www.researchgate.net/profile/ Cynthia Ebinger/publication/248241176 Tectonic model of the Malawi rift Africa/links/5510168c0cf2752610a1d976.pd, 215–235.

Haselwimmer, C., & Prakash, A. (2013). Thermal Infrared Remote Sensing of Geothermal Systems. In C. Kuenzer & S. Dech (Eds.), *Thermal Infrared Remote Sensing* (Vol. 17, pp. 453–473). Dordrecht: Springer Netherlands. doi:10.1007/978-94-007-6639-6

Ray, G. E. (1975). *The Geology of the Chitipa - Karonga Area* (unpublished) (p. 101). Bulletin No 42. Malawi Geological Survey Library, Zomba, Malawi.

Ulusoy, İ., Labazuy, P., & Aydar, E. (2012). STcorr: An IDL code for image based normalization of lapse rate and illumination effects on nighttime TIR imagery. *Computers & Geosciences*, *43*, 63–72. doi:10.1016/j.cageo.2012.02.012.